IEEE TRANSACTIONS ON

MAGNETICS

A PUBLICATION OF THE IEEE MAGNETICS SOCIETY

JULY 2014 VOLUME 50 NUMBER 7 IEMGAQ (ISSN 0018-9464)

PART I OF TWO PARTS

SELECTED PAPERS FROM THE ASIA-PACIFIC DATA STORAGE CONFERENCE 2013

Hualien, Taiwan, November 20–22, 2013

PAPERS

IEEE

Injection Locking of Spin-Torque Nano-Oscillators

Chong Long Cao[1], Yan Zhou[2], Lijun Jiang[1], and Philip W. T. Pong[1]

[1]Department of Electrical and Electronic Engineering, The University of Hong Kong, Hong Kong
[2]Department of Physics, The University of Hong Kong, Hong Kong

We demonstrated the phase locking of a spin-torque oscillator (STO) to an alternating current (ac) using macrospin and micromagnetic simulations. We found that the locking properties of both approaches agree with each other. The phase difference between the STO and the injected ac stabilizes at $\Delta\phi \approx 90°$ and is not sensitive to the initial phase difference, which provides potential application of STO for microwave generation.

***Index Terms*—Injection locking, microwave generator, spin-transfer torque.**

I. Introduction

THE INVESTIGATIONS of current-induced magnetization excitation in magnetic nanopillars have received tremendous interest since the spin-transfer phenomenon was first predicted in the theoretical studies of Berger [2] and Slonczewski [3] in the late 1990s. It has been shown that a spin-polarized direct current (dc) through a free ferromagnetic layer can exert a torque on the magnetic moment of the free layer and flip its magnetization when the spin current exceeds a certain critical value [1]–[3]. Krivorotov *et al.* [4] have experimentally demonstrated that a spin-polarized dc can cause transition to steady precessional modes with typical frequencies at gigahertz under external applied field, leading to the so-called spin-torque oscillator (STO).

Although STO is a possible solution to replace the current microwave generator because it does not need LC tanks, the dependency on the external field and the weak output power (typically below 1 nW) need to be solved to achieve compatibility with the existing microwave circuits. Some attempts have been made on STO to achieve zero external field operation. Houssameddine *et al.* [5] used an STO with a perpendicularly polarized Co/Pt multilayer (perpendicular STO) as the fixed layer and it was shown to generate microwave oscillations at zero applied field. Boulle *et al.* [6] experimentally achieved zero field microwave generation of STO by employing wavy angular dependence of the torque. To enhance the output power, the most investigated route is to phase lock a phase-coherent STO array. Kaka *et al.* [7] and Mancoff *et al.* [8] first demonstrated synchronized oscillation at nanoscale independently: the phase locking of two STOs in close proximity through the spin-wave interaction. Grollier *et al.* [9] have theoretically studied the synchronization of many oscillators in an electrically connected network. In this configuration, synchronization relies on phase locking between the STOs and their self-generated alternating current (ac) [10]–[12]. Ruotolo *et al.* [13] also reported the interaction of magnetic vortices through the mediation of antivortices, leading to synchronization when they are closely spaced. More recently,

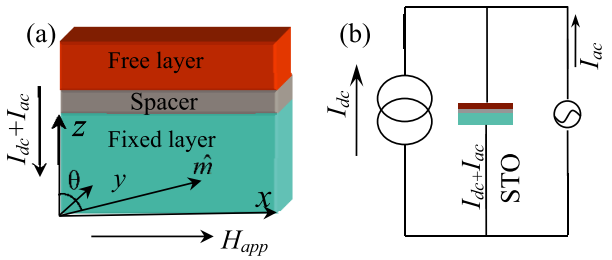

Fig. 1. (a) Sketch of the single STO consisting of a nonmagnetic spacer layer sandwiched between a fixed ferromagnetic layer and a free ferromagnetic layer, and the corresponding coordinate system employed in this paper. x–y plane is the easy plane, with x-axis being the easy axis in the film plane. The free layer magnetization $\boldsymbol{m}$ makes an angle θ with the z-axis. The current I is defined as positive when the negative electrons flow from the fixed layer to the free layer. (b) Schematic view of STO coupled to a dc and an ac.

Petit-Watelot *et al.* [14] reported that a vortex can achieve self-phase locking of its internal gyrotropic mode and the relaxation mode.

In this paper, we have studied the locking behavior of STO using macrospin and micromagnetic approach, respectively. This paper is organized as follows. In Section II, we describe the general approach of Landau–Liftshitz–Gilbert–Slonczewski (LLGS) modeling and the simulated electronic circuit. In Section III, we present the results of the macrospin simulation and then the micromagnetic simulation. The overall summary of these analytical and simulation results are presented in Section IV and we point out that the results provide not only a useful perspective of understanding the STO phase-locking mechanism from the fundamental physics point of view, but also guidelines for optimizing the device performance in realistic applications.

II. Modeling of Injection Locking

As shown in Fig. 1(a), the STO is a typical trilayer system consisting of a thick magnetically fixed layer, nonmagnetic spacer layer, and a thin free (sensing) layer. The injection locking circuit is shown in Fig. 1(b). The time evolution of the free-layer magnetization $\hat{m}$ is found from a numerical solution

Manuscript received October 21, 2013; revised December 12, 2013; accepted December 13, 2013. Date of current version July 7, 2014. Corresponding author: P. W. T. Pong (e-mail: ppong@eee.hku.hk).

Color versions of one or more of the figures in this paper are available online at http://ieeexplore.ieee.org.

Digital Object Identifier 10.1109/TMAG.2013.2295411

of the LLGS equation [1], [2]

$$\frac{d\hat{m}}{dt} = -|\gamma|\hat{m} \times \mathbf{H}_{\text{eff}} + \alpha\hat{m} \times \frac{d\hat{m}}{dt} + |\gamma|\frac{\eta(I_{\text{dc}} + I_{\text{ac}})}{2\mu_0 M_S e V_f}\hat{m} \times (\hat{m} \times \hat{M}) \quad (1)$$

where $\hat{m}$ is the unit vector along the magnetization of the free layer, $\hat{M}$ is the unit vector along the magnetization of the fixed layer, γ is the gyromagnetic ratio, α is the damping coefficient, μ_0 is the magnetic vacuum permeability, η is the spin-transfer efficiency, M_S is the free layer saturation magnetization, and V_f is the volume of the free layer. $\mathbf{H}_{\text{eff}} = H_{\text{app}}\hat{e}_x + H_k(\hat{m} \cdot \hat{e}_x)\hat{e}_x - H_d(\hat{m} \cdot \hat{e}_z)\hat{e}_z$ is the effective magnetic field acting on the free layer, which includes the applied in-plane (IP) magnetic field H_{app}, the uniaxial magnetic anisotropy field H_k, and the out-of-plane (OOP) demagnetization field H_d. $\hat{e}_x$ and $\hat{e}_z$ are the unit vectors along x (IP easy axis) and z (OOP), respectively. For the dependence of the resistance R of the STO on the angle between the magnetization of fixed and free layer at time t, we assume the following standard equation:

$$R(t) = \left\{ \frac{R_P + R_{\text{AP}}}{2} - \frac{R_{\text{AP}} - R_P}{2}\cos(\psi(t)) \right\} \quad (2)$$

where R_P and R_{AP} are the parallel and antiparallel resistances separately. $\psi(t)$ is the angle between the magnetization of the fixed layer and the free layer.

We consider an STO coupled to a dc I_{dc} and an ac I_{ac} [Fig. 1(b)]. To study the shape deviation of small STO samples due to the lithography limitations in realistic fabrication process, we assume a standard deviation in the STO shape anisotropy fields. As shown in Fig. 1(b), the total current flowing through the STO is the summation of the dc and ac, $I_{\text{STO}} = I_{\text{dc}} + I_{\text{ac}}$. I_{dc} drives the STO into dynamic precession, while I_{ac} modulates the oscillation leading to the phase locking.

III. Simulation Result

In a typical IP Co/Cu/Co nanopillars, the fixed layer magnetization $\mathbf{M} = (\mathbf{M}, \mathbf{0}, \mathbf{0})$ lies along the easy axis (x-axis) in the easy plane (x–y plane). The following parameters are adopted in our simulation [9], [15]–[17]: $\alpha = 0.007$, $\gamma = 1.85 \times 10^{11}$ Hz/T, $M_S = 1.27 \times 10^8$ A/m, $\eta = 0.35$, $H_{\text{app}} = 0.2$ T, $H_d = 1.6$ T, $R_P = 10\ \Omega$, and $R_{AP} = 11\ \Omega$. The anisotropy field of the free layer of STO H_k is kept at 0.05 T.

Fig. 2 shows the macrospin simulation results. In Fig. 2(a), we show the precession frequency versus the driving dc. When the driving dc I_{dc} exceeds a critical value, $\hat{m}$ starts its precession in a clam-shell mode, which is also called IP mode, and the precession frequency $f(I_{\text{dc}})$ decreases with I_{dc} (red shift). The STO switches from IP mode to OOP oscillation when I_{dc} continues increasing, and $f(I_{\text{dc}})$ increases with I_{dc} (blue shift). The magnetization precesses following the orbits in the inset of Fig. 2(a). The energy of the system conserves after each precession period because of the closed orbit [18], [19]. The preferred phase shift $\Delta\phi$ is shown in Fig. 2(b). In the inset, we plot a single simulation run when

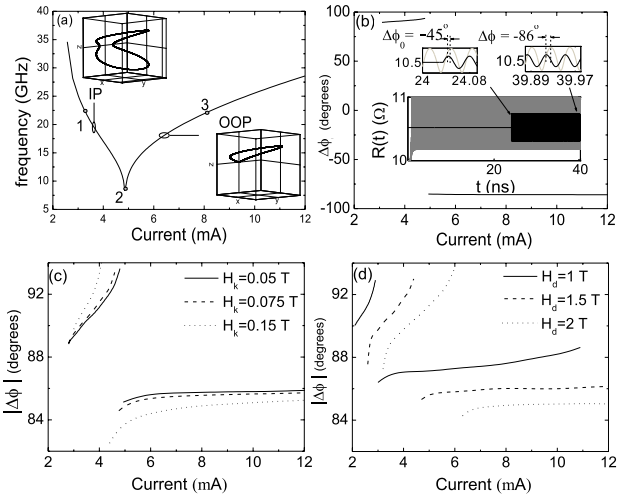

Fig. 2. (a) Typical IP STO precession frequency versus drive current. The insets show the precessional trajectory of the STO for different oscillation modes: IP and OOP. (b) Relative phase shift $\Delta\phi$ between the ac and the STO versus dc drive. Inset: a typical simulation run, which illustrates how the STO locks to its injection ac. (c) Absolute value of preferred phase shift $|\Delta\phi|$ versus dc for different anisotropy field H_k. (d) Demagnetization field H_d tunability of the preferred phase shift $|\Delta\phi|$.

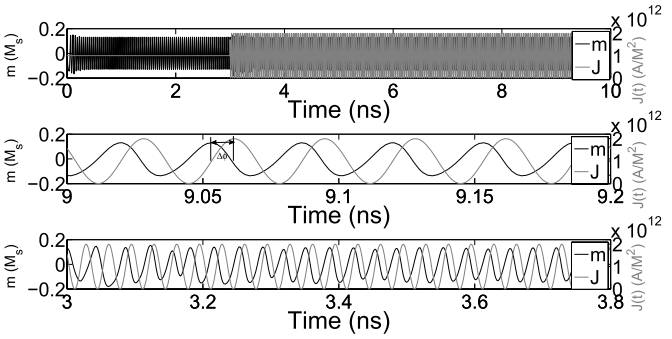

Fig. 3. Micromagnetic simulation of injection locking. The dc density is $J_{\text{dc}} = 10^{12}$ A/m^2, the dimension of the STO is $20 \times 20 \times 2$ nm^3, the initial phase difference between ac and STO is $\Delta\phi_0 \approx 0°$. The top layer is the overall simulation, the middle layer is the transient detail at steady state, and the bottom layer is the transient detail when ac is applied.

$f_{\text{STO}} = 27.7$ GHz, $I_{\text{dc}} = 11.4$ mA, and $I_{\text{ac}} = 22.8\ \mu$A. The upper left figure shows the STO resistance and I_{ac} versus time on the onset of application of ac with an initial phase difference $\Delta\phi_0 = -45°$, and the upper right figure shows the preferred intrinsic phase difference of $\Delta\phi = -86°$ at the steady state. The dc dependence of the preferred phase difference $\Delta\phi$ can be further fine tuned by varying the anisotropy field [Fig. 2(c)] and demagnetization field [Fig. 2(d)] of the sample. The preferred phase difference at around 90° can be explained by the orbit energy conservation over one period in steady states when considering the ac, which has been discussed in [18].

To compare with our macrospin results and have a better understanding on the preferred phase difference in the framework of the micromagnetism, we perform the micromagnetic simulations for the injection locking using the OOMMF micromagnetic package [20] and the spin-transfer-torque extension module [21]. Due to the calculation capacity,

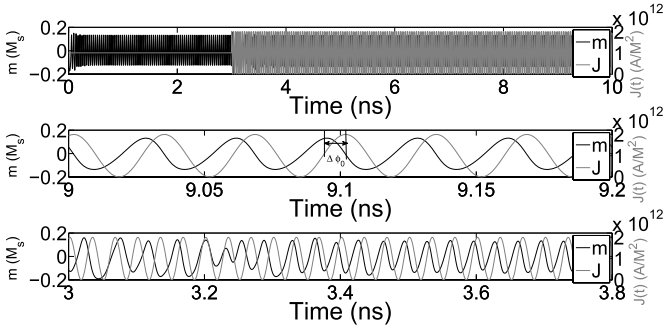

Fig. 4. Micromagnetic simulation of injection locking. The dc density is $J_{\rm dc} = 10^{12}$ A/m^2, the dimension of the STO is $20 \times 20 \times 2$ nm^3, and the initial phase difference between ac and STO is $\Delta\phi_0 \approx 180°$. The top layer is the overall simulation, the middle layer is the transient detail at steady state, and the bottom layer is the transient detail when ac is applied.

we chose a relatively small dimension of the STO for simulation. As shown in Figs. 3 and 4, the initial phase difference between the injected ac and the STO is 0° and 180°, respectively. We can see that the phase difference finally stabilizes at $\Delta\phi \approx 90°$, regardless of the initial phase difference, which agrees with the macrospin simulations.

IV. Conclusion

In summary, we have studied the phase-locking characteristics of a free-running STO under an external ac employing both macrospin and micromagnetic simulation. We observe a phase shift of about 90° in both approaches, in line with the predictions from our analytical analysis. The phase difference at steady state is not sensitive to the initial phase difference between the STO and the ac. This property provides useful information for achieving synchronization of multiple STOs.

Acknowledgment

This work was supported in part by the Seed Funding Program for Basic Research and Small Project Funding Program from the University of Hong Kong, in part by ITF Tier 3 funding under Grant ITS/112/12, in part by RGC-GRF under Grant HKU 704911P, and in part by the University Grants Committee of Hong Kong under Contract AoE/P-04/08.

References

[1] J. C. Slonczewski, "Current-driven excitation of magnetic multilayers," *J. Magn. Magn. Mater.*, vol. 159, nos. 1–2, pp. L1–L7, Jun. 1996.

[2] L. Berger, "Emission of spin waves by a magnetic multilayer traversed by a current," *Phys. Rev. B*, vol. 54, no. 13, pp. 9353–9358, Oct. 1996.

[3] J. C. Slonczewski, "Excitation of spin waves by an electric current," *J. Magn. Magn. Mater.*, vol. 159, no. 2, pp. L261–L268, May 1999.

[4] I. N. Krivorotov, N. C. Emley, J. C. Sankey, S. I. Kiselev, D. C. Ralph, and R. A. Buhrman, "Time-domain measurements of nanomagnet dynamics driven by spin-transfer torques," *Science*, vol. 307, no. 5707, pp. 228–231, Jan. 2005.

[5] D. Houssameddine, U. Ebels, B. Delaet, B. Rodmacq, I. Firastrau, F. Ponthenier, *et al.*, "Spin-torque oscillator using a perpendicular polarizer and a planar free layer," *Nature Mater.*, vol. 6, no. 6, pp. 447–453, Jun. 2007.

[6] O. Boulle, V. Cros, J. Grollier, L. G. Pereira, C. Deranlot, F. Petroff, *et al.*, "Shaped angular dependence of the spin-transfer torque and microwave generation without magnetic field," *Nature Phys.*, vol. 3, no. 7, pp. 492–497, Jul. 2007.

[7] S. Kaka, M. R. Pufall, W. H. Rippard, T. J. Silva, S. E. Russek, and J. A. Katine, "Mutual phase-locking of microwave spin torque nano-oscillators," *Nature*, vol. 437, no. 7057, pp. 389–392, Sep. 2005.

[8] F. B. Mancoff, N. D. Rizzo, B. N. Engel, and S. Tehrani, "Phase-locking in double-point-contact spin-transfer devices," *Nature*, vol. 437, no. 7057, pp. 393–395, 2005.

[9] J. Grollier, V. Cros, and A. Fert, "Synchronization of spin-transfer oscillators driven by stimulated microwave currents," *Phys. Rev. B*, vol. 73, no. 6, pp. 060409-1–060409-4, 2006.

[10] W. H. Rippard, M. R. Pufall, S. Kaka, T. J. Silva, S. E. Russek, and J. A. Katine, "Injection locking and phase control of spin transfer nano-oscillators," *Phys. Rev. Lett.*, vol. 95, no. 6, p. 067203, 2005.

[11] L. Dong, Y. Zhou, Z. Chang-Song, and H. Bam-Bi, "Fractional locking of spin-torque oscillator by injected ac current," *Phys. Rev. B*, vol. 83, no. 17, pp. 174424-1–174424-8, 2011.

[12] Y. Zhou, V. Tiberkevich, G. Consolo, E. Iacocca1, B. Azzerboni, A. Slavin, *et al.*, "Oscillatory transient regime in the forced dynamics of a nonlinear auto-oscillator," *Phys. Rev. B*, vol. 82, no. 1, pp. 012408-1–012408-4, 2010.

[13] A. Ruotolo, V. Cros, B. Georges, A. Dussaux, J. Grollier, C. Deranlot, *et al.*, "Phase-locking of magnetic vortices mediated by antivortices," *Nature Nanotechnol.*, vol. 4, no. 8, pp. 528–532, Aug. 2009.

[14] S. Petit-Watelot, J.-V. Kim, A. Ruotolo, R. M. Otxoa, K. Bouzehouane, J. Grollier, *et al.*, "Commensurability and chaos in magnetic vortex oscillations," *Nature Phys.*, vol. 8, no. 9, pp. 682–687, Sep. 2012.

[15] S. I. Kiselev, J. C. Sankey, I. N. Krivorotov, N. C. Emley, R. J. Schoelkopf, R. A. Buhrman, *et al.*, "Microwave oscillations of a nanomagnet driven by a spin-polarized current," *Nature*, vol. 425, no. 6956, pp. 380–383, 2003.

[16] J. Xiao, A. Zangwill, and M. D. Stiles, "Macrospin models of spin transfer dynamics," *Phys. Rev. B*, vol. 72, no. 1, pp. 014446-1–014446-13, 2005.

[17] H. Xi, Z. Lin, and A. M. Wilomowski, "Understanding the current-induced magnetization dynamics in the presence of large magnetic fields," *J. Magn. Magn. Mater.*, vol. 296, no. 1, pp. 32–36, Jan. 2006.

[18] Y. Zhou, J. Persson, S. Bonetti, and J. Ä. Kerman, "Tunable intrinsic phase of a spin torque oscillator," *Appl. Phys. Lett.*, vol. 92, no. 9, pp. 092505-1–092505-3, Mar. 2008.

[19] Y. Zhou, J. Persson, and J. Ä. Kerman, "Intrinsic phase shift between a spin torque oscillator and an alternating current," *J. Appl. Phys.*, vol. 101, no. 9, pp. 09A510-1–09A510-3, May 2007.

[20] M. Donahue and D. Porter. (2013, Sep. 10). *The Object Oriented MicroMagnetic Framework (OOMMF) Project at ITL/NIST* [Online]. Available: http://math.nist.gov/oommf/

[21] C.-Y. You. (2013, Sep. 10). *Spin Transfer Torque (STT) Extension Module for OOMMF(Object Oriented MicroMagnetic Framework)* [Online]. Available:http://spintronics.inha.ac.kr/STT-OOMMF.html